Alteration of TiC in Supernovae Outflows: Transmission Electron Microscopy Study of TiC Subgrains in Supernovae Graphite. T. L. Daulton[1,2], T. J. Bernatowicz[3,2], and T. K. Croat[3,2], [1]Center for Materials Innovation, [2]Physics, [3]Laboratory for Space Sciences, Washington University in St. Louis, St. Louis MO 63130, USA.

Introduction:

Primitive carbonaceous chondrites contain within their matrices micron-sized presolar graphite spherules [1]. In Murchison, the majority of the graphite spherules are of asymptotic giant branch (AGB) star origin and are generally of high density [2.15-2.20 g/cm^3] with a mean diameter of ~ 2 μm while those of supernovae (SN) origin are generally of low density [1.65-1.72 g/cm^3] with a mean diameter of ~ 6 μm [2]. Embedded within the graphite spherules are 7-500 nm TiC (often in solid solution with V, Zr, Mo, and Ru at upwards of 20 at.% although occasionally carbides with < 2 at.% Ti have been observed) as well as 10-80 nm Fe-Ni metal kamacite and taenite subgrains that were undoubtedly incorporated during graphite condensation [2-5]. While both AGB and SN graphite spherules contain TiC, the metal subgrains have so far only been observed in SN graphites (often attached to TiC). In SN graphites, measured mass abundances of carbide and metal subgrains range from 25-2400 ppm (corresponding to 1-1000 subgrains per spherule).

These high-temperature condensates were evidently ubiquitous in their respective gas outflows at regions of graphite formation, and their microstructures record valuable information on chemical and physicial conditions present within the relatively short window between their formation and subsequent encapsulation [2]. Once shielded within the interior of the graphite spherules, these subgrain microstructures survived largely unaltered, protected from subsequent chemical processing in the interstellar media and solar nebula.

Alteration Processes in Supernovae Outflows:

Transmission Electron Microscopy (TEM) studies of cross-sectioned SN graphite spherules suggest TiC grains were altered in the SN outflows prior to capture [3-5]. Many TiC grains exhibit subhedral morphologies suggesting that primary growth faces were weathered or corroded. Furthermore, between ~ 6% to 50% of the total TiC population in some SN graphite spherules exhibited evidence of a 3-15 nm thick rim along a portion or entire length of the TEM projected perimeter of the grains; and similar rims were also observed on some metal grains [4,5]. Importantly, neither the grain morphology nor the presence/lack of a rim correlated with the spatial proximity of the TiC grains to the surface of the graphite spherules, indicating these features were primary microstructures developed prior to the incorporation of the subgrains into the host graphite.

Two possible grain alteration mechanisms have been proposed for rim formation in SN outflows: a) particle irradiation due to collisions between grains and gas moving at different relative velocities (reminiscent of rim formation on lunar soil grains by solar wind) and/or b) chemical corrosion from exposure to reactive gas species following grain growth [4,5]. To establish the mechanism responsible for rims and provide constraints on physical conditions in SN grain forming regions we are performing detailed TEM microcharacterizations on subgrains and their rim structures. We report some preliminary findings here.

Results & Discussion:

High-resolution TEM images of rimmed TiC SN grains exhibit phase contrast that suggests amorphous and poorly crystalline grain surfaces (Fig. 1). It is important to note that TEM images are two-dimensional projections of three-dimensional objects. In Fig. 1, the TiC grain (i.e., cross-sectional plane) was tilted 11.6° (± 15° uncertainty in the plane of the cross section) relative to the electron beam. If the TEM projection plane is tilted with respect to the normal of an interface, an abrupt interface between two phases would appear as a wide band of superimposed phases.

While some TiC grains do exhibit rims that appear fully amorphous, several points suggest the rim in Fig. 1 is not a tilted projection of a grain with a purely amorphous surface layer. The rim thickness (4.7 nm) is relatively small (i.e., not tilt broadened) compared to the range observed (3-15 nm) and the image contrast at the rim interface is relatively abrupt (i.e., not a continuous gradation). Furthermore, a wide variation

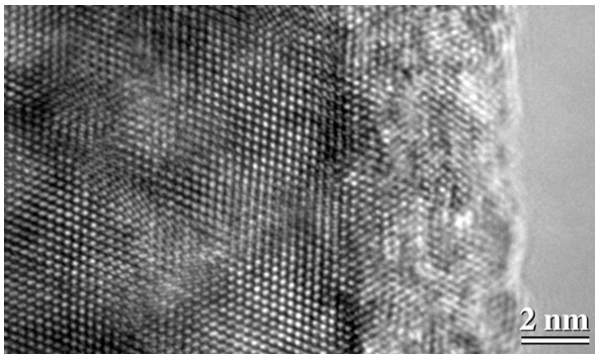

Fig. 1. High-resolution TEM phase contrast image along the [011] crystallographic axis of a perimeter region of a rimmed TiC that separated from the host graphite matrix during ultramicrotome sectioning.

in apparent degree of amorphization is observed in the rim along the perimeter of grain and the rims are electron beam sensitive to amorphization. The existence of rims with poor crystallinity and instability to electron irradiation suggest the presence of relatively high densities of strain fields.

High angle annular dark field (HAADF) Scanning (S)-TEM imaging (Fig. 2) supported by STEM-electron energy loss spectroscopy (EELS) thickness maps (Fig. 3) demonstrate voids in rimmed TiC. In HAADF, images are formed using electrons that scattered through high angles (in our case, 37-128 mR). The cross section for high-angle scattering is approximately proportional to the square of the mean atomic number, resulting in contrast dependent on mass density. The HAADF images show nm-sized regions of depleted mass density that dynamically evolve and grow under high-dose electron beam exposure. Growth of these voids demonstrates a large density of vacancy defects in the lattice.

Large densities of lattice defects in the rims and in proximity to the rims suggest irradiation damage, possibly resulting from differential velocity collisions between dust and H gas in the SN outflow. Furthermore, unlike chemical corrosion, irradiation is consistent with the observation of rims on chemically dissimilar phases within SN graphites. Intriguingly, formation of nm-sized H bubbles have been observed in synthesized SiC [6] and TiC [7] irradiated by $> 10^{17}$ H_2^+/cm^2, and bubbles were observed to develop during subsequent electron irradiation [6]. Therefore, the voids that evolve under electron irradiation that we observe in presolar TiC could represent H bubbles.

Although data for TiC are lacking, measured range profiles of 1 keV He ions (250 eV/nucleon) into SiC peak at 6.7 nm (full width at half maximum span 0-13 nm) [8], consistent with observed rim thicknesses. Assuming rims formed by H irradiation, an order-of-magnitude estimate of 250 eV for the H energies represents a differential velocity between TiC dust and H gas of 220 km/s in SN outflows. In comparison, SN outflow velocities have been estimated at 25,800 ± 1,200 km/s from γ-ray burst observations [9]. It is reasonable to expect fluctuations in outflow velocities of the order of ±1%. Such fluctuations would be comparable to differential velocities between dust and H gas needed to produce grain rims.

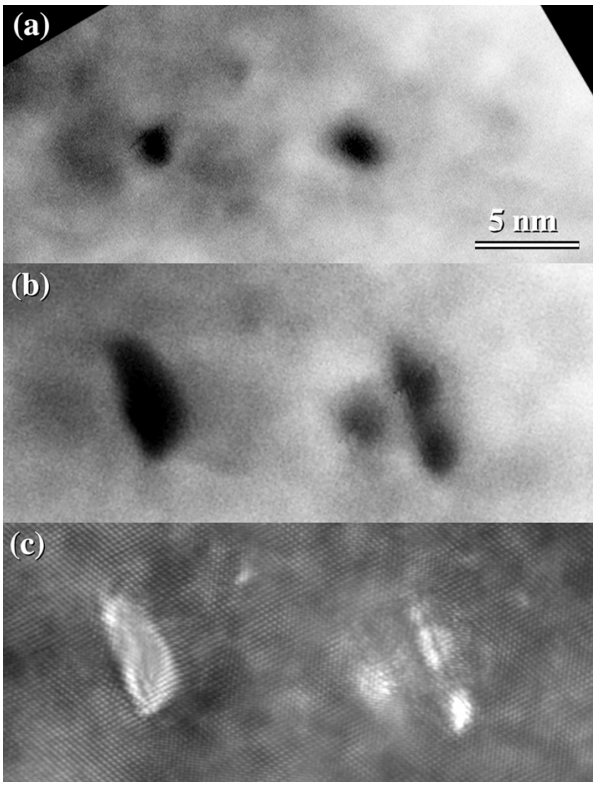

Fig. 2. Region of TiC grain 75 ± 5 nm from a surface rim (*importantly*, void distance from a surface rim in direction normal to the cross-section plane is unknown). HAADF STEM *z*-contrast images a) before and b) after high-dose electron exposure (dark contrast reflects lower mass density); c) High-resolution TEM phase contrast image along the [011] crystallographic axis (corresponding to same structure as in panel b) showing evidence of strain fields and several voids with a facet on a {311} plane.

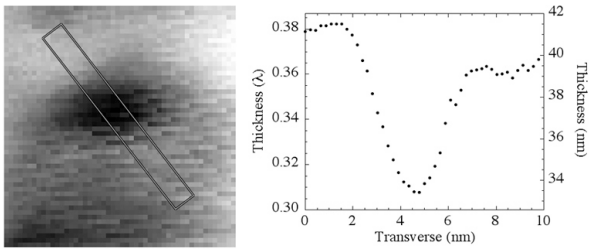

Fig. 3. STEM-EELS thickness map of rightmost void/bubble in Fig. 2a. Decreasing thickness corresponds to darker contrast. A transverse is shown at the right in terms of effective electron mean-free path (λ for 200 keV electrons scattered ≤ 22.7 mR) and absolute nm.

References: [1] Amari S. et al. (1994) *Geochim. Comoschim. Acta*, 58, 459-470. [2] Bernatowicz T. J. et al. (2006) in *Meteorites and the Early Solar System II*, eds D. Lauretta & H. Y. McSween Jr., (U. of Arizona Press), 109-126. [3] Bernatowicz T. J. et al. (1991) *Astrophys. J.*, 373, L73-L76. [4] Bernatowicz T. J. et al. (1999) *LPSC XXX*, 1392. [5] Croat T. K. et al. (2003) *Geochim. Comoschim. Acta*, 67, 4705-4725. [6] Hojou K. et al. (1991) *J. Elec. Micr.*, 40, 157-161. [7] Hojou K. et al. (1996) *J. Nucl. Mat.*, 239, 279-283. [8] Miyagawa S. et al. (1984) *Jap. J. Appl. Phys.*, 23, 1380-1384. [9] Reeves J. N. et al. (2002) *Nature*, 416, 512-515.